

## Catalytic oxidative desulfurization of dibenzothiophene by heterogeneous $M^{2+}/Al$ -layered double hydroxide ( $M^{2+} = Zn, Mg, Ni$ ) modified zinc oxide

Nur Ahmad<sup>a</sup>, Nova Yuliasari<sup>a</sup>, Fitri Suryani Arsyad<sup>b</sup>, Idha Royani<sup>b</sup>, Risfidian Mohadi<sup>a,c</sup>, Aldes Lesbani<sup>a,c\*</sup>

a) Graduate School of Mathematics and Natural Sciences, Faculty of Mathematics and Natural Sciences, Universitas Sriwijaya, Jl. Palembang Prabumulih Km.32 Ogan Ilir 30662, Indonesia

b) Department of Physics, Faculty of Mathematics and Natural Sciences, Universitas Sriwijaya, Jl. Palembang Prabumulih Km.32 Ogan Ilir 30662, Indonesia

c) Research Center of Inorganic Materials and Coordination Complexes, Faculty of Mathematics and Natural Sciences, Universitas Sriwijaya, Jl. Palembang Prabumulih Km.32 Ogan Ilir 30662, Indonesia

Received 9 September 2022; received in revised form 16 December 2022; accepted 31 January 2023 (DOI:10.30495/IJC.2023.1972458.1973)

### ABSTRACT

In this study, the preparation of layered double hydroxide-metal oxide (ZnAl-ZnO, MgAl-ZnO, and NiAl-ZnO) was successful. The characterization of the catalyst used XRD, FTIR, and SEM analysis. The catalyst shows high oxidative desulfurization of dibenzothiophene. The percentage conversion of dibenzothiophene on ZnAl-ZnO, MgAl-ZnO, and NiAl-ZnO was 99.38%, 99.34%, and 99.90%, respectively. The acidities of ZnAl-ZnO, MgAl-ZnO, and NiAl-ZnO were 0.798, 2.469, and 0.184 mmol/g, respectively. The catalysts are heterogeneous systems, and the advantage is that they can be used for reusability. After 3 cycles of catalytic reactions at 323 K for 30 min, reusability proves that the percentage conversion of dibenzothiophene on ZnAl-ZnO, MgAl-ZnO, and NiAl-ZnO had a stable structure.

**Keywords:** Dibenzothiophene, Heterogeneous catalyst, layered double hydroxide, Oxidative desulfurization, Reusability

### 1. Introduction

Currently, the development of the vehicle industry is increasing. Most of the vehicles produced still use fossil fuels. However, fossil fuels containing sulfur compounds are one of the causes of air pollution [1]. Therefore, sulfur compounds such as dibenzothiophene and its derivatives must be converted to dibenzothiophene-sulfones [2]. In 2005, Europe permitted a sulfur concentration of 10 ppm in fuel oil; however, in 2006, America permitted a sulfur concentration of 15 ppm [3], [4]. The desulfurization methods being developed, such as biodesulfurization (BDS) [5], adsorptive desulfurization [6], extractive desulfurization (EDS) [7], and oxidative desulfurization [8]–[10]. The oxidative desulfurization method is a current concern in oxidizing dibenzothiophene compounds and their derivatives.

Conventional hydrodesulfurization is used to reduce the content of sulfur compounds, but it requires high temperatures and pressure [11]. Oxidative desulfurization does not require high temperatures to convert dibenzothiophene, so it is very effective [12]. The oxidative desulfurization process requires a catalyst to increase the reaction rate [13]. The development of catalysts for the desulfurization process is still being carried out until now [14]. Catalysts for oxidative desulfurization of dibenzothiophenes such as polyoxometalates [15], Cr-promoted sulfated zirconia [16], Mo/MCM-41 [17], and layered double hydroxide (LDH) [18], [19].

LDH is a compound composed of a positively charged layer and an anion interlayer [20]. The Chemical composition of the constituent layers, layer charge density, type of anion, the quantity of anions, and the size of LDH can be modified [21]. In oxidative desulfurization processes, LDH has good prospects as a catalyst. Catalysis is of importance to LDH because of

\*Corresponding author:

E-mail address: aldeslesbani@pps.unsri.ac.id  
(A. Lesbani)

its large surface area and thermal stability [22]. LDH is combined with ZnO, a metal oxide, to increase the active site in oxidative desulfurization. ZnO catalyst is low-cost and has a high oxidizing capacity [23], [24]. ZnO has gained a great deal of interest in the degradation and oxidation of environmental pollutants [25], [26]. Calcinating LDH and metal oxide combination produce produces composites easily [27]. LDH has been reported for catalysis processes, such as photocatalytic [28], [29], methanol electrooxidation [30], and hydrogen production [31]. There are homogeneous and heterogeneous catalysts. Homogeneous catalysts are soluble in the reaction's reactants and/or products, whereas heterogeneous catalysts are insoluble. The benefit of heterogeneous catalysts is their reusability [32].

ZnAl-ZnO, MgAl-ZnO, and NiAl-ZnO were produced as catalysts for the oxidative desulfurization of dibenzothiophene in this study. To determine the success of catalyst preparation, XRD, FTIR, and SEM analyses were employed to characterize catalysts. Variations were made to time, UV-Vis spectrum, catalyst dosage, temperature, solvent, acidity test, and reusability in order to optimize the oxidative desulfurization of dibenzothiophene. The heterogeneous test was conducted to see whether a really heterogeneous system would be produced.

## 2. Experimental

### 2.1. Preparation of layered double hydroxide-zinc oxide

ZnAl-ZnO, MgAl-ZnO, and NiAl-ZnO were prepared according to previously reported methods by Ahmad et al. [33]: 0.75 M magnesium/zinc/nickel nitrate hexahydrate and 0.25 M aluminum nitrate nonahydrate dissolved in 100 mL of pure water, stirred for 10 min. Then slowly add 2 M sodium hydroxide to pH 10. The mixture was stirred for 10 h at 353 K, then added ZnO (ratio 1:1), and shaken for 3 h. the mixture was added 150 mL 0.37 M sodium hydroxide, shaken for 10 h at 353 K, filtered, dried, and then calcinated at 573 K for 7 h.

### 2.2. Characterization

Characterization of the materials using an X-Ray Diffractometer (Rigaku Miniflex-6000), UV-Vis Spectrophotometer (EMC-18PC-UV), Fourier Transfer Infra-Red (Shimadzu Prestige-21), and Scanning Electron Microscope (Quanta 650).

### 2.3. Oxidative desulfurization and analysis

Catalytic oxidative desulfurization reactions were carried out in a 100 mL two-pronged flask under magnetic stirring at 300 rpm and connected with a condenser. 500 ppm as the initial concentration of

dibenzothiophene was added to 30 mL of n-hexane as a solvent, followed by 0.25 g of ZnAl-ZnO, MgAl-ZnO, and NiAl-ZnO. 1 mL hydrogen peroxide and 3 mL acetonitrile were added as oxidant and extraction agents, respectively. The reaction was set at 323 K and observed per 10 min. The sulfur conversion of dibenzothiophene was analyzed by equation (1).

$$\% \text{ conversion} = \frac{(C_0 - C_f)}{C_0} \times 100 \quad (1)$$

Where,  $C_0$  and  $C_f$  are the initial and final concentrations of dibenzothiophene, respectively.

### 2.4. Heterogeneous test

A heterogeneous test was conducted by desulfurizing 500 ppm of dibenzothiophene in 30 mL of n-hexane at 323 K for 10 min. Afterward, the catalyst and dibenzothiophene solution was separated. The dibenzothiophene solution continued with the desulfurization process for 20-30 min at 323 K. The sulfur conversion of dibenzothiophene was analyzed.

## 3. Results and Discussion

Diffraction patterns of ZnAl-ZnO, MgAl-ZnO, and NiAl-ZnO are shown in **Fig. 1**. The catalysts peaks were detected at  $2\theta = 10.29^\circ, 31.75^\circ, 34.41^\circ, 36.24^\circ, 47.52^\circ, 56.56^\circ,$  and  $60.16^\circ$  corresponding to the (003), (100), (002), (101), (002), (110), and (013) reflections, respectively. The diffraction peaks at  $2\theta = 10.29^\circ$  and  $60.16^\circ$  indicate the typical structure of LDH [34]. The diffraction peaks at  $2\theta 31.75^\circ, 34.41^\circ, 36.24^\circ, 47.52^\circ, 56.56^\circ$  indicate typical structure of ZnO. JCPDS of ZnAl, MgAl, NiAl, and ZnO were in accordance with numbers 138-0486, 22-700, 15-0087, and 36-1451, respectively [35], [36]. The crystallite size was determined by using Scherrer's equation for the XRD data. Equation (2) illustrates the Scherrer equation [37].

$$d = (K \times \lambda) / (\beta \times \cos \theta) \quad (2)$$

The Scherrer equation verifies the relationship between crystallite size  $d$  (nm) and  $\beta$  (peak width of the diffraction peak or FWHM) and  $\cos \theta$  (the half of the diffraction angle). In addition, it demonstrates that the term  $d$  has a direct relationship with the Scherrer constant  $K$  (often 0.9, depending on the crystallite shape) and the X-ray wavelength  $\lambda$  (Cu-K $\alpha$  line at 0.15406 nm) [38]. Based on the Scherrer equation, ZnAl-ZnO, MgAl-ZnO, and NiAl-ZnO have average crystallite sizes of 22, 30, and 25 nm, respectively.

The FTIR spectrum (**Fig. 2**) of ZnAl-ZnO, MgAl-ZnO, and NiAl-ZnO shows characteristic vibrations at 3398,

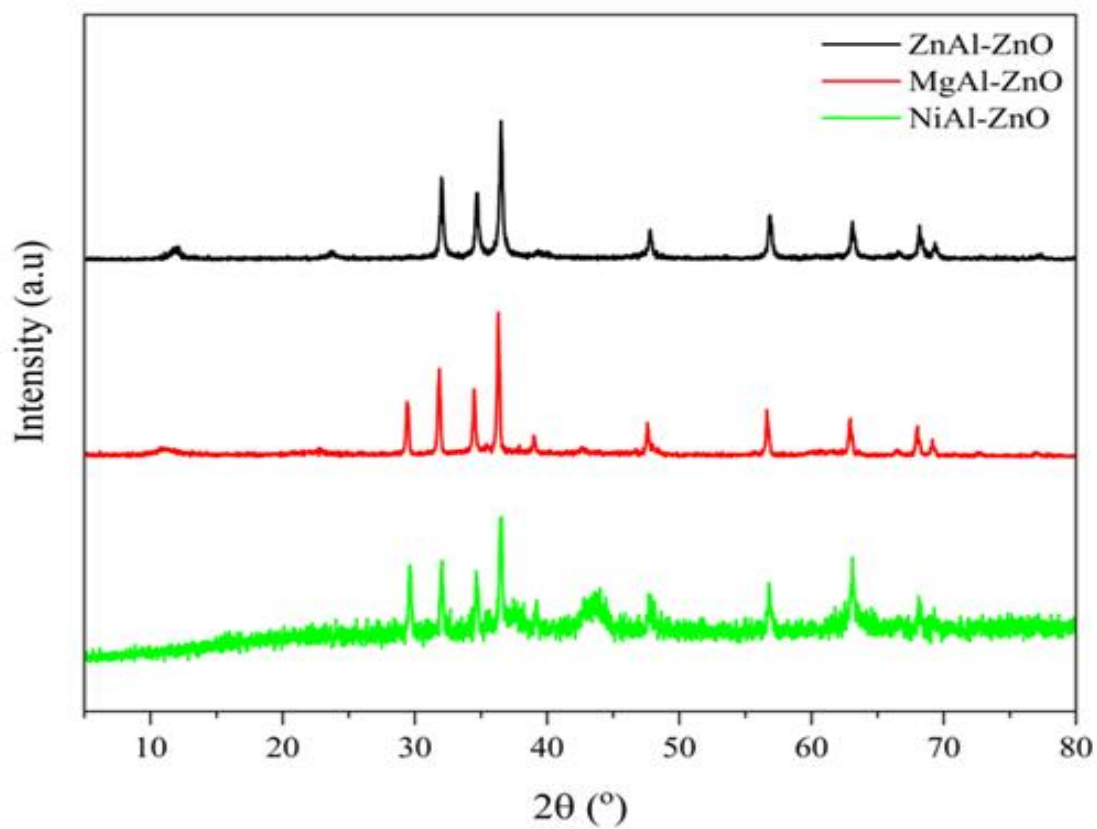


Fig. 1 Diffraction lines of catalysts

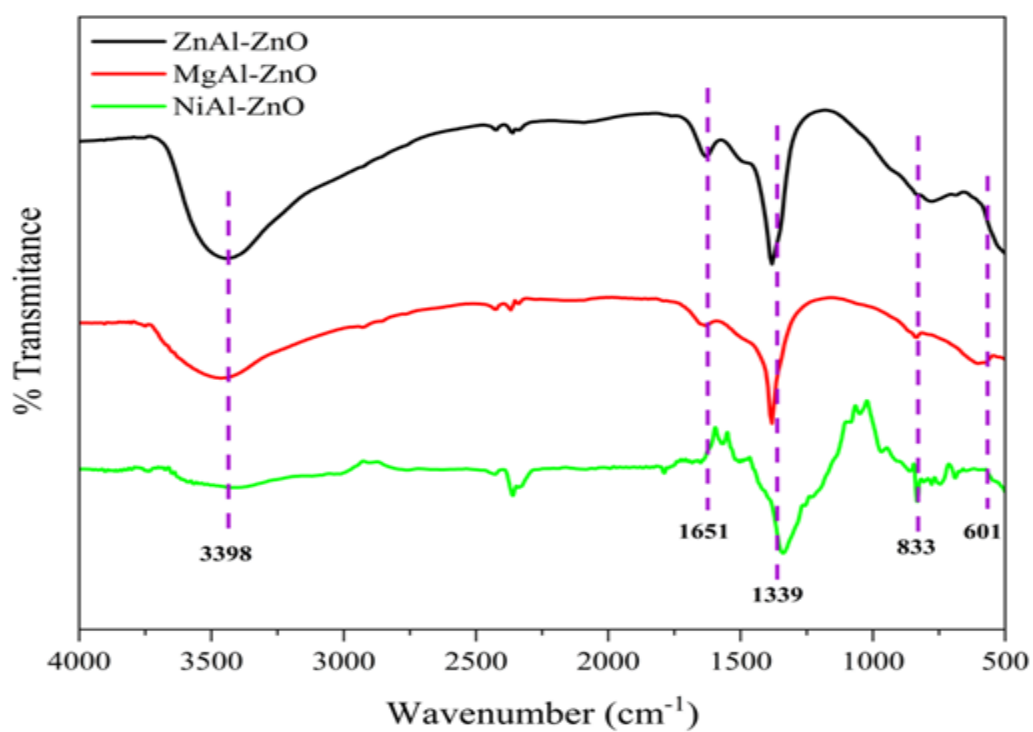


Fig. 2 FTIR spectra of catalysts

1651, 1339, 833, and 601  $\text{cm}^{-1}$ . The peak at 3398  $\text{cm}^{-1}$  could be correlated to O-H stretching [39]. 1651 and 1339  $\text{cm}^{-1}$  correspond to H-O-H and  $\text{NO}_3^-$  stretching from LDH [40]. Metal oxide in LDH and ZnO was observed at 833 and 601  $\text{cm}^{-1}$  [29]. The M-O and M-O-M absorption peaks between ZnO and LDH overlap at 833 and 601  $\text{cm}^{-1}$ .

The surface morphology and diameter distribution of ZnAl-ZnO, MgAl-ZnO, and NiAl-ZnO are depicted in Fig. 3. The usual surfaces of ZnAl-ZnO, MgAl-ZnO, and NiAl-ZnO are not smooth and have uneven forms and sizes. ZnAl-ZnO, MgAl-ZnO, and NiAl-ZnO have average diameter distributions of 2.8 nm, 51.0 nm, and 28.5 nm, respectively. ZnAl-ZnO possessed a narrower diameter distribution than MgAl-ZnO and NiAl-ZnO.

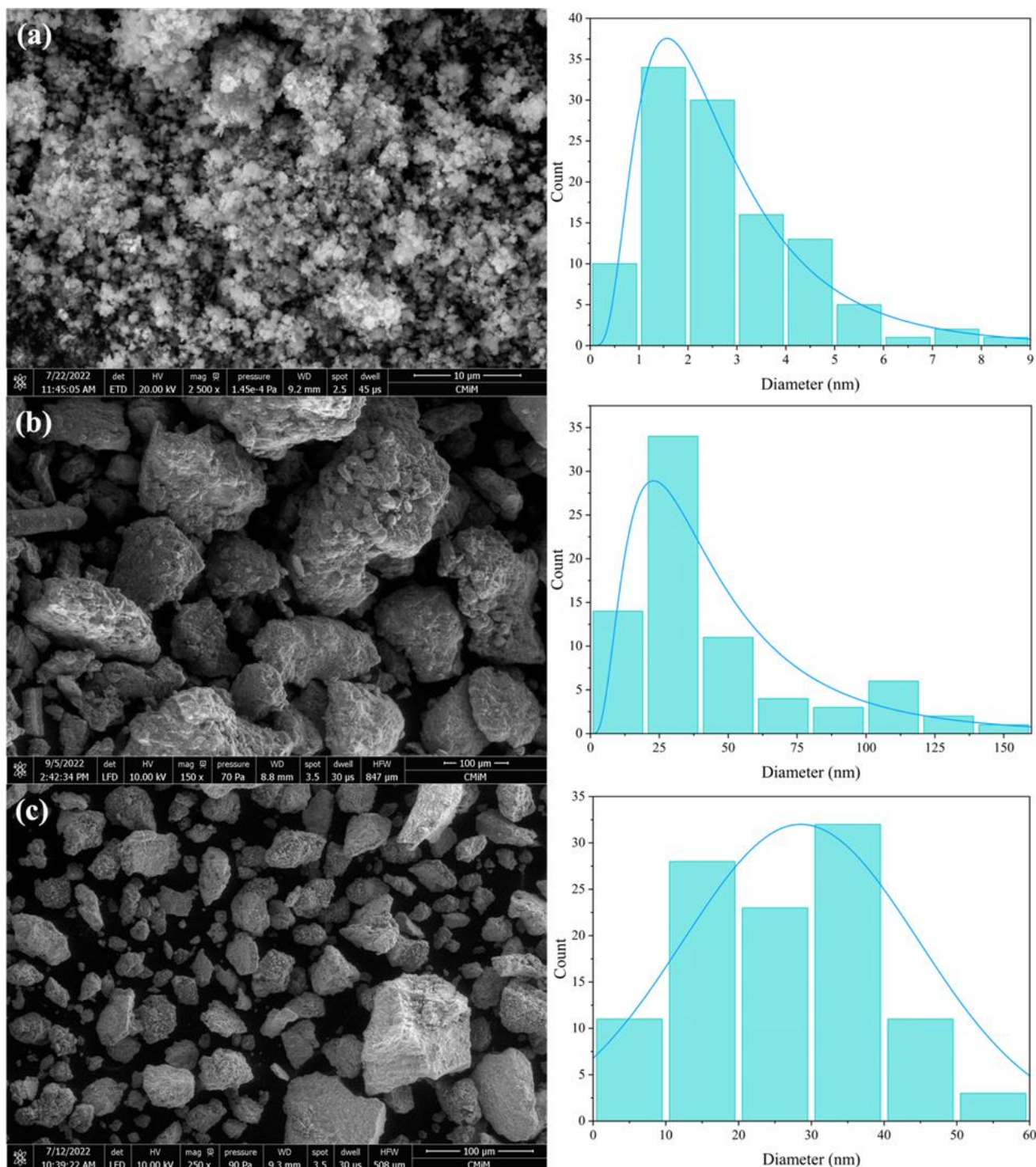


Fig. 3 SEM pictures and diameter distribution of ZnAl-ZnO (a), MgAl-ZnO (b), and NiAl-ZnO (c)

Pyridine served as the adsorbate base for the acidity test of ZnAl-ZnO, MgAl-ZnO, and NiAl-ZnO. The acidity of ZnAl-ZnO, MgAl-ZnO, and NiAl-ZnO, according to **Table 1**, was 0.798, 2.469, and 0.184 mmol/g, respectively. The amount of pyridine adsorbed influences the acidity of catalysts. During oxidative desulfurization, acid sites are able to take electrons. To convert dibenzothiophene to dibenzothiophene-sulfones, the acid sites of catalysts must be polyacid [41]. The positively charged LDH ( $\text{Zn}^{2+}$ ,  $\text{Mg}^{2+}$ ,  $\text{Ni}^{2+}$ ,  $\text{Al}^{3+}$ ) can generate a strong electrostatic field, which can easily activate the hydrogen atoms in H-bonds and release protons, hence increasing the number of strong Bronsted acid sites. Transition metal cations of LDH have the ability to generate Lewis acid sites. Schematic oxidative desulfurization of dibenzothiophene is displayed in **Fig. 4**.

In the oxidative desulfurization of dibenzothiophene, reaction time is one of the most influential elements of conversion. **Fig. 5** depicts the 10-60 min reaction time used. The increase in reaction time enhances the dibenzothiophene conversion in catalysts. Increasing reaction time improves the interaction between two immiscible phases, enhancing efficiency [33]. For 500 ppm dibenzothiophene, the ZnAl-ZnO, MgAl-ZnO, and

NiAl-ZnO conversion rates were 99.38%, 99.34%, and 99.90%, respectively. The optimal response time was 30 min.

The 220-250 nm wavelength scan desulfurization technique was utilized. **Fig. 6** demonstrates that the maximum wavelength of dibenzothiophene is 235 nm. The absorbance of dibenzothiophene dropped as the reaction time increased. As an oxidizing agent,  $\text{H}_2\text{O}_2$  is essential for converting dibenzothiophene to dibenzothiophene-sulfones [42], [43]. In the final step of the oxidative desulfurization process, acetonitrile was utilized as an extraction agent to remove oxidized sulfur compounds [44].

**Table 1.** Acidity of catalyst

Catalyst	Acidity (mmol/g)
Zn/Al-ZnO	0.798
Mg/Al-ZnO	2.469
Ni/Al-ZnO	0.184

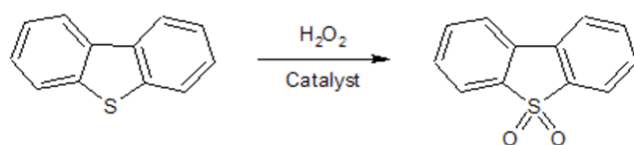


**Fig. 4** Schematic Oxidative desulfurization of dibenzothiophene

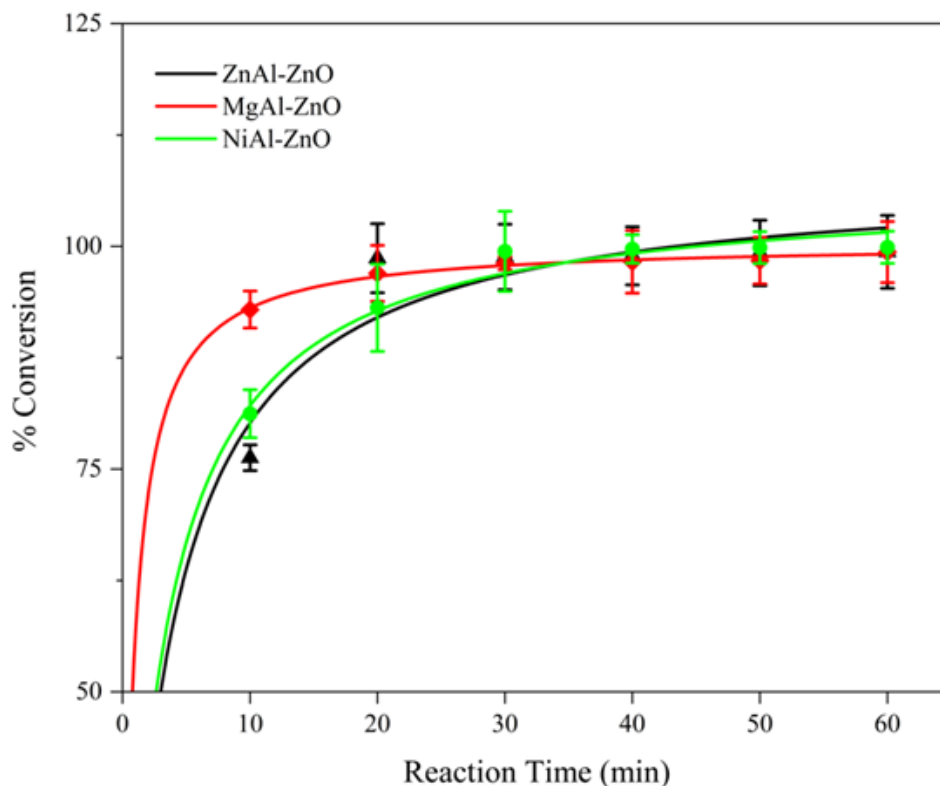


**Fig. 5** Effect of reaction time on oxidative desulfurization of dibenzothiophene (n-hexane solvent, 0.25 g catalysts, 323 K, 300 rpm)

Variations of 0.05, 0.1, 0.25, 0.5, and 1 g were used to examine the influence of catalyst dose on the oxidative desulfurization of dibenzothiophene. At a temperature of 323 K for 30 min, the effect of catalyst dosage was investigated for an initial concentration of 500 ppm dibenzothiophene. Based on the findings in **Fig. 7**, 0.25 g of ZnAl-ZnO, MgAl-ZnO, or NiAl-ZnO is the optimal amount of catalyst for the desulfurization of dibenzothiophene. The increase in catalyst dosage increases the catalytic site and the competition with oxidant molecules [16], [45].

Temperature-dependent oxidative desulfurization of dibenzothiophene at 303 K to 323 K. Based on **Fig. 8**,

the optimal desulfurization temperature for dibenzothiophene is 323 K. Temperature increase accelerates the rate of molecular diffusion and increases the interaction between dibenzothiophene and catalysts, so making the desulfurization process successful [9]. Consequently, the oxidative desulfurization procedure is set to 323 K. In addition, n-pentane, n-hexane, and n-heptane were utilized as solvents for dibenzothiophene. In terms of solvent effect, n-hexane is superior to n-pentane and n-heptane. **Fig. 9** depicts the conversion of dibenzothiophene on MgAl-ZnO < ZnAl-ZnO < NiAl-ZnO. This study compared several published studies shown in **Table 2**.

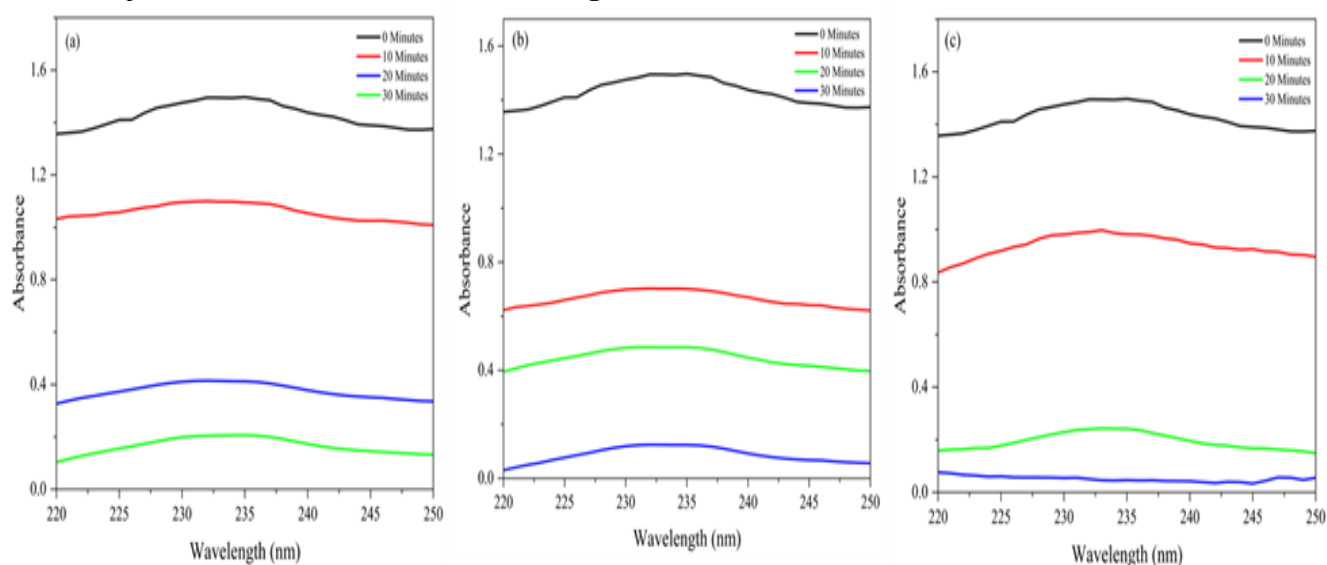


**Fig. 6** UV-Vis spectrum of oxidative desulfurization dibenzothiophene by ZnAl-ZnO (a), MgAl-ZnO (b), and NiAl-ZnO (c) (n-hexane solvent, 0.25 g catalysts, 323 K, 300 rpm)

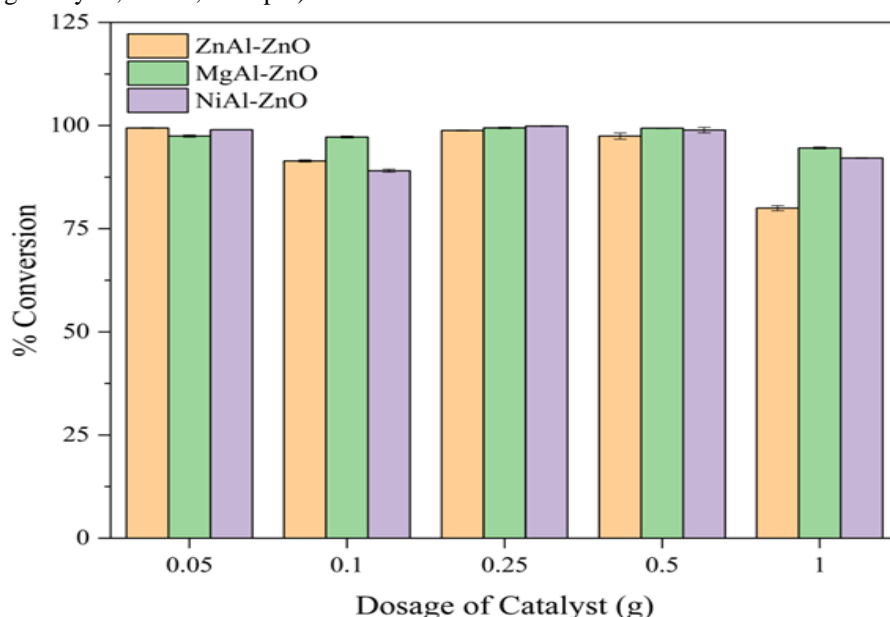


**Fig. 7** Variation dosage of catalysts (n-hexane solvent, 30 min, 323 K, 300 rpm)

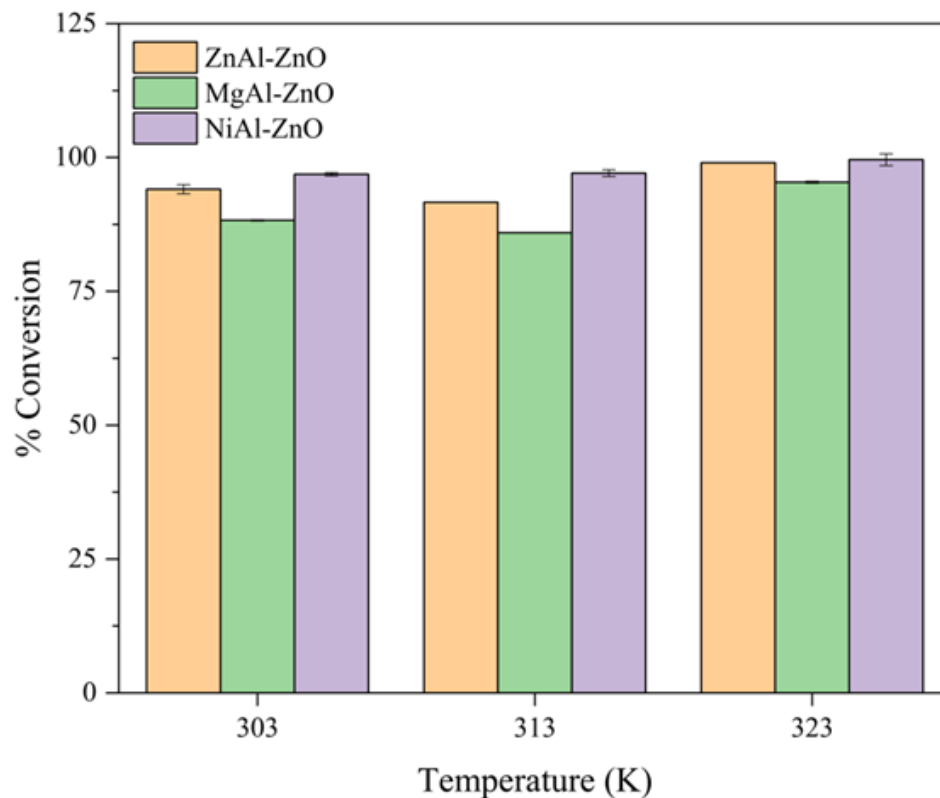


**Fig. 8** Effect of temperatures on oxidative desulfurization by composite catalysts (n-hexane solvent, 0.25 g catalysts, 30 min, 300 rpm)

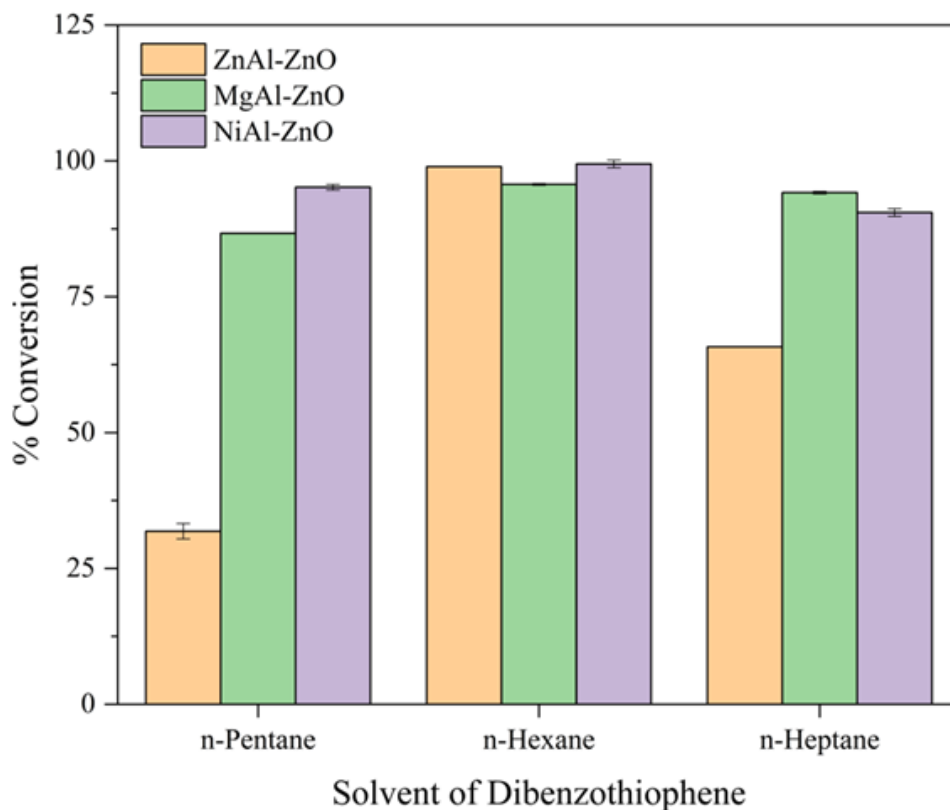


**Fig. 9** Effect of solvent on desulfurization of dibenzothiophene by composite catalysts (30 min, 0.25 g catalysts, 323 K, 300 rpm)

**Table 2.** Comparison this work with several published studies

Catalyst	Reaction conditions	% Conversion of dibenzothiophene	Ref.
ZnO-AC	t = 120 min, T = 333 K, dosage of catalyst = 0.1 g, solvent = n-hexane, oxidant = H <sub>2</sub> O <sub>2</sub> , DBT = 500 ppm	93.83	[41]
Mo/Ti-PILC	t = 30 min, T = 373 K, dosage of catalyst = 0.005 g, solvent = n-octane, oxidant = CYHPO, DBT = 500 ppm	99.90	[48]
WO <sub>3</sub> /TiO <sub>2</sub>	t = 60 min, T = 323 K, dosage of catalyst = 0.15 g, solvent = n-octane, oxidant = H <sub>2</sub> O <sub>2</sub> , DBT = 800 ppm	100	[49]
MDC-C	t = 120 min, T = 353 K, dosage of catalyst = 0.02 g, solvent = n-octane, oxidant = H <sub>2</sub> O <sub>2</sub> , DBT = 1000 ppm	99.50	[50]
BaFe <sub>2</sub> O <sub>4</sub>	t = 120 min, T = 303 K, dosage of catalyst = 0.1 g, solvent = n-octane, oxidant = H <sub>2</sub> O <sub>2</sub> , DBT = 500 ppm	92	[51]
ZnAl-ZnO	t = 30 min, T = 323 K, dosage of catalyst = 0.25 g, solvent = n-hexane, oxidant = H <sub>2</sub> O <sub>2</sub> , DBT = 500 ppm	99.38	This study
MgAl-ZnO	t = 30 min, T = 323 K, dosage of catalyst = 0.25 g, solvent = n-hexane, oxidant = H <sub>2</sub> O <sub>2</sub> , DBT = 500 ppm	99.34	This study
NiAl-ZnO	t = 30 min, T = 323 K, dosage of catalyst = 0.25 g, solvent = n-hexane, oxidant = H <sub>2</sub> O <sub>2</sub> , DBT = 500 ppm	99.90	This study

Homogeneous or heterogeneous tests were conducted to determine whether ZnAl-ZnO, MgAl-ZnO, and NiAl-ZnO are catalysts. The catalyst and dibenzothiophene were separated after undergoing an oxidative desulfurization process at 323 K for 10 min. Without a catalyst, the reaction lasted between 20 and 30 min. The constant concentration of dibenzothiophene suggests that the system is heterogeneous. In accordance with **Fig. 10**, ZnAl-ZnO, MgAl-ZnO, and NiAl-ZnO are heterogeneous catalysts. The benefit of heterogeneous catalysts can be applied to reusability processes [32].

The reusability of the catalyst is crucial for the industry's cost-cutting efforts [46]. Using n-hexane as the solvent, the reusability of catalysts was examined. After each cycle, the recovered catalyst is ultrasonically desorbed, dried, and reused in oxidative desulfurization [47]. **Fig. 11** exhibited the catalyst's reusability after three cycles. After three cycles of oxidative desulfurization, dibenzothiophene conversion on ZnAl-ZnO, MgAl-ZnO, and NiAl-ZnO was 89.71%, 96.02%, and 98.99%, respectively. The capacity to be reused demonstrates that ZnAl-ZnO, MgAl-ZnO, and NiAl-ZnO have stable structures. In order to bolster this claim, FTIR analysis

was performed to detect changes in functional groups. **Fig. 12** demonstrates that the FTIR spectrum of dibenzothiophene before and after oxidative desulfurization did not change considerably. The spectra of ZnAl-ZnO, MgAl-ZnO, and NiAl-ZnO have observed at 3398, 1651, 1339, 833, and 601 cm<sup>-1</sup>. Metal oxide in LDH and ZnO was observed around 833 and 601 cm<sup>-1</sup>. Therefore, the ZnAl-ZnO, MgAl-ZnO, and NiAl-ZnO composites have a stable structure and can be reused.

#### 4. Conclusions

In this study, ZnAl-ZnO, MgAl-ZnO, and NiAl-ZnO were successfully prepared. The catalyst demonstrates high oxidative desulfurization of dibenzothiophene. The percentage of dibenzothiophene conversion on ZnAl-ZnO, MgAl-ZnO, and NiAl-ZnO, respectively, was 99.38%, 99.34%, and 99.90%. Catalysts are heterogeneous systems, with the benefit being their reusability. Reusability demonstrates that the structure of dibenzothiophene on ZnAl-ZnO, MgAl-ZnO, and NiAl-ZnO remained stable after three cycles of catalytic reactions.

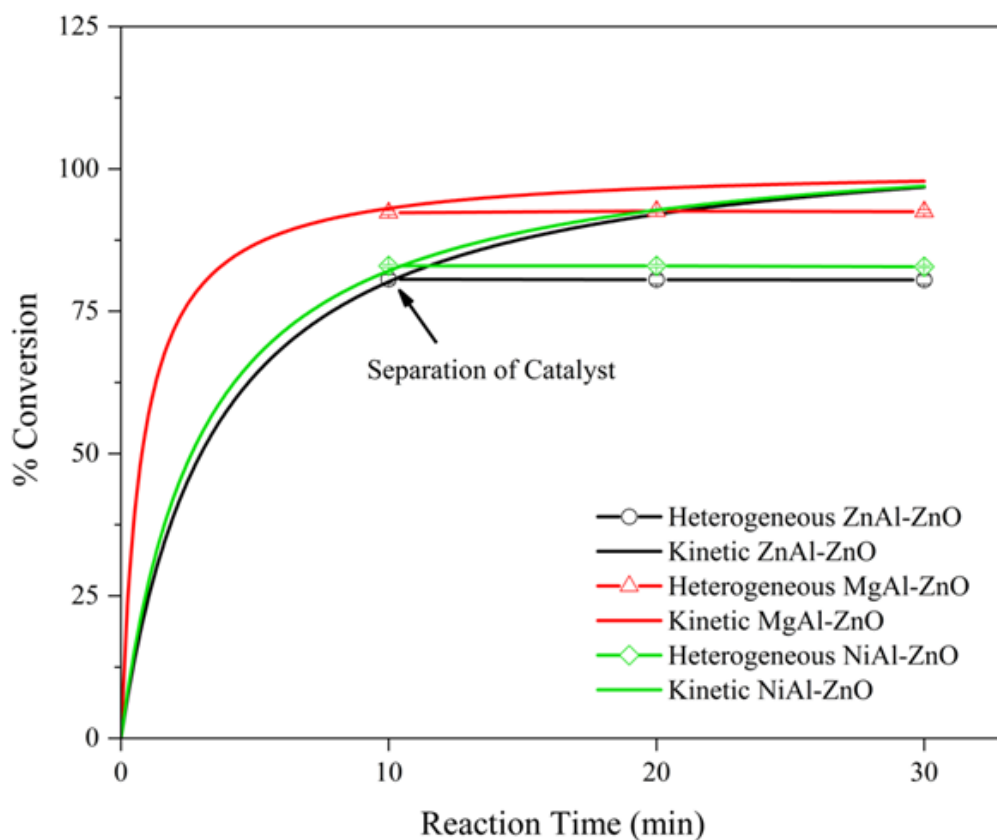


**Fig. 10** Heterogeneous test of catalysts (n-hexane solvent, 0.25 g catalysts, 323 K, 300 rpm)

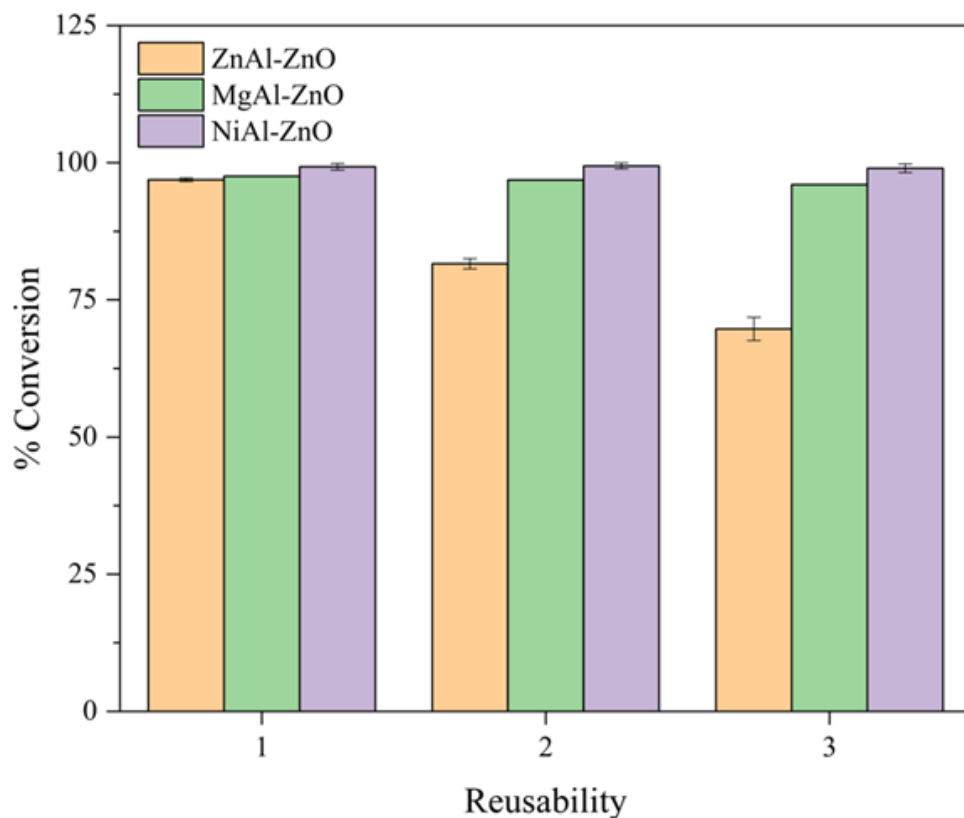


**Fig. 11** Reusability experiments of catalysts (n-hexane solvent, 0.25 g catalysts, 323 K, 300 rpm)

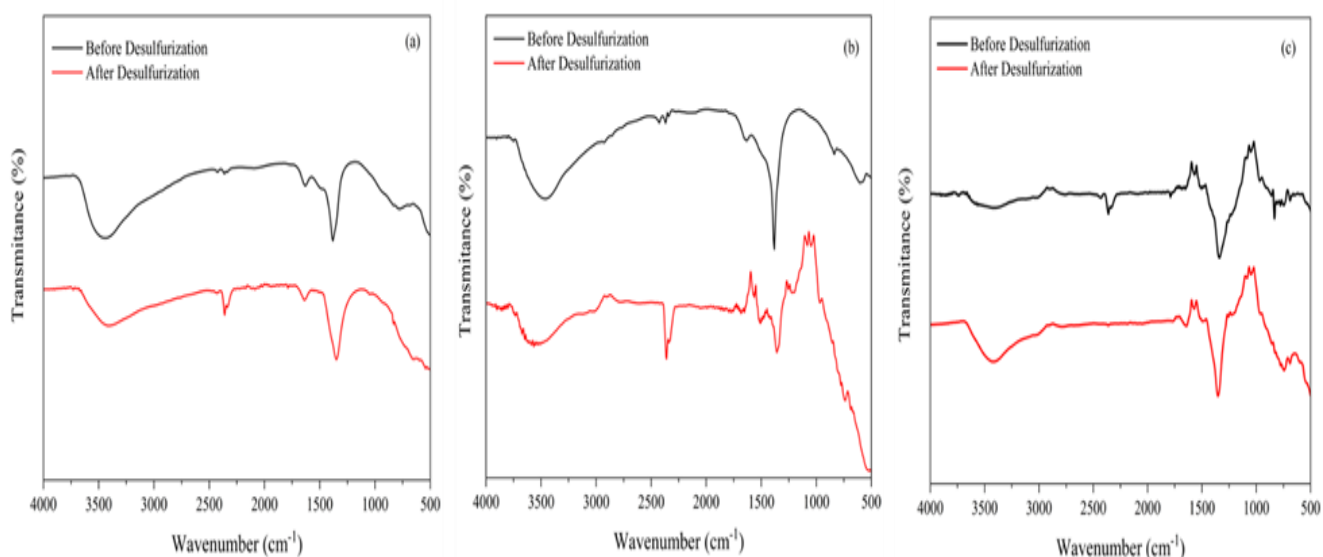


**Fig. 12** FTIR spectra of Zn/Al-ZnO (a), Mg/Al-ZnO (b), Ni/Al-ZnO (c) after the third cycles oxidative desulfurization proces

### Acknowledgements

Authors express gratitude to Universitas Sriwijaya for funding this research through DIPA of Public Service Agency of Universitas Sriwijaya, Hibah Profesi SIP DIPA-023.17.2.677515/2022 on December 12, 2021, by the Rector degree number 0111/UN9.3.1/SK/2022 on April 28, 2022, as additional output. We thank the Research Center of Inorganic Materials and Complexes at Universitas Sriwijaya for their instrumental analyses and constructive discussions.

### References

- [1] X. N. Pham, B. M. Nguyen, H. T. Thi, H. van Doan, *Adv. Pow.Tech.* 29 (2018) 1827–1837.
- [2] S. Mgidlana, T. Nyokong, *Inor. Chim. Acta.* 514 (2021) 119970.
- [3] A. Bazyari, A. A. Khodadadi, A. H. Mamaghani, J. Beheshtian, L. Thompson, and Y. Mortazavi, *Appl. Catal. B.* 180 (2015) 65-77.
- [4] X. Ren, G. Miao, Z. Xiao, F. Ye, Z. Li, H. Wang, J. Xiao, *Fuel.* 174 (2016) 118-125.
- [5] R. S. Malani, A. H. Batghare, J. B. Bhasarkar, V. S. Moholkar, *Bioresour. Tech. Rep.* 14 (2021) 100668.
- [6] S. Subhan, A. U. Rahman, M. Yaseen, H. U. Rashid, M. Ishaq, M. Sahibzada, Z. Tong, *Fuel.* 237 (2019) 793–805.
- [7] M. Rezaee, F. Feyzi, M. R. Dehghani, *J. Mol. Liq.* 333 (2021) 115991.
- [8] N. Kayedi, A. Samimi, M. A. Bajgirani, A. Bozorgian, *S. Afr. J. Chem. Eng.* 35 (2021) 153–158.

- [9] Y. Cao, H. Wang, R. Ding, L. Wang, Z. Liu, B. Lv, *Appl. Catal. A. Gen.* 589 (2020) 117308.
- [10] M. E. Manríquez-Ramírez, M. T. Valdez, L. v. Castro, M. E. Flores, E. Ortiz-Islas, *Mater. Res. Bull.* 153 (2022) 111864.
- [11] F. Abedini, S. Allahyari, N. Rahemi, *Appl. Surf. Sci.* 569 (2021) 151086.
- [12] V. Mahmoudi, A. M. Kermani, M. Ghahramaninezhad, A. Ahmadpour, *Molecular. Catalysis.* 509 (2021) 111611.
- [13] M. L. Luna, M. A. Taboada-Ortega, M. A. Alvarez-Amparán, L. Cedeño-Caero, *Catal. Today.* 394-396 (2022) 336-347.
- [14] H. Naseri, G. Mazloom, A. Akbari, F. Banisharif, *Micro. Meso. Mat.* 325 (2021) 111341.
- [15] H. Yang, B. Jiang, Y. Sun, X. Tantai, X. Xiao, J. Wang, L. Zhang, *Molecular. Catalysis.* 448 (2018) 38–45.
- [16] S. Kumar, V. C. Srivastava, R. P. Badoni, *Fuel. Processing. Technol.* 93 (2012) 18–25.
- [17] P. Sikarwar, U. K. A. Kumar, V. Gosu, V. Subbaramaiah, *J. Environ. Chem. Eng.* 6 (2018) 1736–1744.
- [18] M. Wu, B. Chang, T. T. Lim, W. da Oh, J. Lei, J. Mi, *J. Hazard. Mater.* 360 (2018) 391–401.
- [19] S. Masoumi, S. A. Hosseini, *Fuel.* 277 (2020) 118137.
- [20] T. Taher, R. Putra, N. R. Palapa, A. Lesbani, *Chem. Phys. Lett.* 777 (2021) 138712.

- [21] L. Xiong, W. de Zhang, Q. S. Shi, A. P. Mai, *Polym. Adv. Tech.* 26 (2015) 495–501.
- [22] X. Zhu, C. Chen, Q. Wang, Y. Shi, D. O’Hare, N. Cai, *Chemical. Eng. J.* 366 (2019) 181–191.
- [23] B. Divband, A. Jodaie, M. Khatmian, *Iranian. J. Catal.* 9 (2019) 63-70.
- [24] F. Iazdani, A. Nezamzadeh-Ejhieh, *Envi. Sci. Poll. Res.* 28 (2021) 53314–53327.
- [25] K. A. Isai, V. S. Shrivastava, *Iranian. J. Catal.* 9 (2019) 259-268.
- [26] S. Ghattavi, A. Nezamzadeh-Ejhieh, *J. Mol. Liq.* 322 (2021) 114563.
- [27] C. Dang, W. Yang, J. Zhou, W. Cai, *Appl. Catal. B.* 298 (2021) 120547.
- [28] A. Elhalil, R. Elmoubarki, A. Machrouhi, M. Sadiq, M. Abdennouri, S. Qourzal, N. Barka, *J. Environ. Chem. Eng.* 5 (2017) 3719–3726.
- [29] S. Intachai, T. Nakato, N. Khaorapapong, *Appl. Clay. Sci.* 201 (2021) 105927.
- [30] E. E. Abdel-Hady, R. Mahmoud, S. H. M. Hafez, H. F. M. Mohamed, *J. Mater. Res. Tech.* 17 (2022) 1922–1941.
- [31] T. Li, L. Tan, Y. Zhao, Y. F. Song, *Chem. Eng. Sci.* 245 (2021) 116839.
- [32] P. Polikarpova, A. Akopyan, A. Shlenova, A. Anisimov, *Catal. Commun.* 146 (2020) 106123.
- [33] N. Ahmad, A. Wijaya, E. S. Fitri, F. S. Arsyad, R. Mohadi, A. Lesbani, *Sci. Tech. Indo.* 7 (2022) 385-391.
- [34] M. Badaruddin, N. Ahmad, E. S. Fitri, A. Lesbani, R. Mohadi, *Sci. Tech. Indo.* 7 (2022) 492-499.
- [35] L. Chen, X. Yang, Y. Tian, Y. Wang, X. Zhao, X. Lei, F. Zhang, *Front. Energy. Res.* 9 (2022) 810568.
- [36] P. Basnet, D. Samanta, T. I. Chanu, J. Mukherjee, S. Chatterjee, *SN. Appl. Sci.* 1 (2019) 633.
- [37] M. Zebardast, A. F. Shojaei, K. Tabatabaeian, *Iranian. J. Catal.* 8 (2018) 297-309.
- [38] A. Noruozi, A. Nezamzadeh-Ejhieh, *Chem. Phys. Lett.* 752 (2020) 137587.
- [39] N. Ahmad, F. S. Arsyad, I. Royani, A. Lesbani, *Results. Chem.* 4 (2022) 100629.
- [40] H. Lv, H. Rao, Z. Liu, Z. Zhou, Y. Zhao, H. Wei, Z. Chen, *J. Energy. Storage.* 52 (2022) 104940.
- [41] W. Trisunaryanti, S. D. Sumbogo, S. A. Novianti, D. A. Fatmawati, M. Ulfa, Y. L. Nikmah, *Bull. Chem. Reac. Eng. Catal.* 16 (2021) 881–887.
- [42] D. Xie, Q. He, Y. Su, T. Wang, R. Xu, B. Hu, *Chinese. J. Catal.* 36 (2015) 1205–1213.
- [43] A. Lesbani, A. Agnes, R. O. Saragih, M. Verawaty, R. Mohadi, H. Zulkifli, *Bull. Chem. Reac. Eng. Catal.* 16 (2015) 185-191.
- [44] A. V. Akopyan, D. A Plotnikov, P. D. Polikarpova, A. A. Kedalo, S. V. Egazar’yants, A. V. Anisimiv, E. A. Karakhanov, *Petro. Chem.* 59 (2019) 975–978.
- [45] L. Qiu, Y. Cheng, C. Yang, G. Zeng, Z. Long, S. Wei, K. Zhao, L. Luo, *RSC. Adv.* 6 (2016) 17036–17045.
- [46] W. Jiang, D. Zheng, S. Xun, Y. Qin, Q. Lu, W. Zhu, H. Li, *Fuel.* 190 (2019) 1–9.
- [47] S. O. Ribeiro, C. M. Granadeiro, P. L. Almeida, J. Pires, M. C. Capel-Sanchez, J. M. Campos-Martin, S. Gago, B. de. Castro, S.S. Balula, *Catal. Today.* 333 (2019) 226–236.
- [48] L. Kang, H. Liu, H. He, C. Yang, *Fuel.* 234 (2018) 1229–1237.
- [49] J. Ye, J. Wen, D. Zhao, P. Zhang, A. Li, L. Zhang, H. Zhang, M. Wu, *Chinese. Chem. Let.* 31 (2020) 2819–2824.
- [50] B. N. Bhadra, J. Y. Song, N. A. Khan, S. H. Jhung, *ACS. Appl. Mater. Interfaces.* 9 (2017) 31192–31202.
- [51] S. Mandizadeh, M. Sadri, M. Salavati-Niasari, *Sep. Puri. Tech.* 175 (2017) 399-405.